

THE SOLAR X-RAY SPECTRUM AND THE DENSITY OF THE UPPER ATMOSPHERE

BY E. T. BYRAM, T. A. CHUBB, AND H. FRIEDMAN

United States Naval Research Laboratory, Washington 25, D.C.

(Received March 12, 1956)

ABSTRACT

The flux density of solar x-rays arriving in the E region of the ionosphere was measured by means of photon counters in rockets. Flux densities as a function of altitude were obtained in the spectral bands 8A to 20A, 44A to 60A, and 44A to 100A. The data were extrapolated to zero air mass to give the respective flux densities in the three bands outside the atmosphere. To a first approximation, the observations may be fitted to a 700,000 deg K Planckian distribution of solar x-rays with a total flux density of about $0.1 \text{ erg cm}^{-2} \text{ sec}^{-1}$ at the earth. A more refined analysis reveals that it is an oversimplification to assign a single temperature to the entire corona. The shortest wavelengths, 8A to 20A, appear to have come from a hotter source, at a temperature between one and two million deg K. From the rate of x-ray absorption between 128 and 110 km and known mass absorption coefficients for air, the atmospheric density was computed to be about one-third the current Rocket Panel average values.

Since radio reflection measurements first revealed strong solar control of the ionosphere, its formation has been attributed to short wavelength ultraviolet and soft x-ray radiations emitted by the chromosphere and corona. The use of high altitude rockets in recent years has made possible the direct measurement of these solar radiations. From the data obtained in early experiments [see 1 and 2 of "References" at end of paper], which were limited to x-ray wavelengths shorter than 20A, it appeared likely that sufficient intensity was available in the complete soft x-ray spectrum below 100A to produce most of the E region. The measurements, begun in 1949, have utilized x-ray photon counters in V-2, Viking, and Aerobee rockets. The results described in this paper are based on NRL Aerobees 14 and 16, primarily the latter, flown from White Sands Proving Ground, New Mexico, in November and December of 1953. These experiments were designed to obtain additional information on the highly variable flux observed in previous flights in the 8 to 20A range and to extend x-ray measurements to longer wavelengths. By using thin plastic windows, the spectral response of the photon counters was extended from the carbon K edge at 43.5A to about 100A. Since a major portion of the solar x-ray emission theoretically is expected to fall in the 40 to 100A range, the new data provide a fairly good estimate of the total x-ray intensity absorbed in E region. The flights occurred at a time of very low solar activity and

correspondingly weak coronal green-line emission. The observed x-ray distribution can be approximated by a 700,000 deg K grey body with a total intensity of about $0.1 \text{ erg cm}^{-2} \text{ sec}^{-1}$ absorbed between 110 and 130 km.

In spite of technical difficulties, it may eventually be possible to obtain the solar spectrum in the soft x-ray region with high resolution by flying a grating spectrograph with photographic or electronic recording, as has been done in the ultraviolet above 1000Å [3, 4]. At the present time, however, the photon-counter technique is the only method that has succeeded in obtaining intensity data with sufficient resolution to outline the broader features of the x-ray end of the coronal spectrum. The design of the photon-counter experiments and the treatment of the rocket data are described in detail below.

It is also possible to use the measurement of x-ray transmission in the atmosphere to compute the air density at E-layer altitudes. For the day of the Aerobee 16 experiment, the ambient pressures in the 110- to 128-km region were found to be about one-third the values listed by the Rocket Panel.

Instrumentation

The x-ray detectors employed in Aerobees 14 and 16 consisted of a group of four types of thin-window photon counters, designed to respond to different wavelength and intensity ranges. These counters looked out the side of the rocket and their signals were telemetered to ground to provide a continuous record of intensity during flight. They showed significant responses only when the rocket roll gave them a direct view of the sun. Except for the detectors, the instrumentation was identical to that described in reference [5].

The least sensitive x-ray detector flown was a counter with a beryllium window, 1/4 inch in diameter and 0.005 inch thick, which did not transmit appreciable x-ray intensity above 8Å. This detector showed no response. All three remaining counters were sensitive to longer wavelengths and measured solar x-rays. The spectral sensitivities of these three counters are shown in Figures 1 and 2. These curves were determined by calculating the window transmission and x-ray absorption in the gas of each counter, with the assumptions that each quantum absorbed in the counting gas caused a Geiger count and that all counts were due to quantum photoelectrically absorbed by the gas. To check the latter assumption, a counter tube filled with 95 percent He and 5 percent ethyl formate was exposed to radiation from an x-ray tube operated at 1500 volts. As the pressure of gas in the counter was decreased, the counting rate diminished. At zero pressure, the extrapolated counting rate was 0.5 percent of that obtained with one atmosphere of gas filling. For longer wavelengths, most of the radiation is absorbed in the first few millimeters of gas and the yield from photoelectric effect at the cathode is entirely negligible.

Since very soft x-rays are absorbed preferentially near the window, it was necessary to check the assumption that each x-ray quantum absorbed in the gas caused a Geiger count. A counter of the type flown was fitted with a window of lithium fluoride and exposed to ultraviolet light containing wavelengths from 1500Å to 2000Å. These wavelengths were shorter than the photoelectric threshold of the cathode, but not short enough to photoionize the gas. Using the tube as a photocell without gas amplification, its photoelectric current was measured. Then the applied voltage was raised to the Geiger region and the counting rate observed.

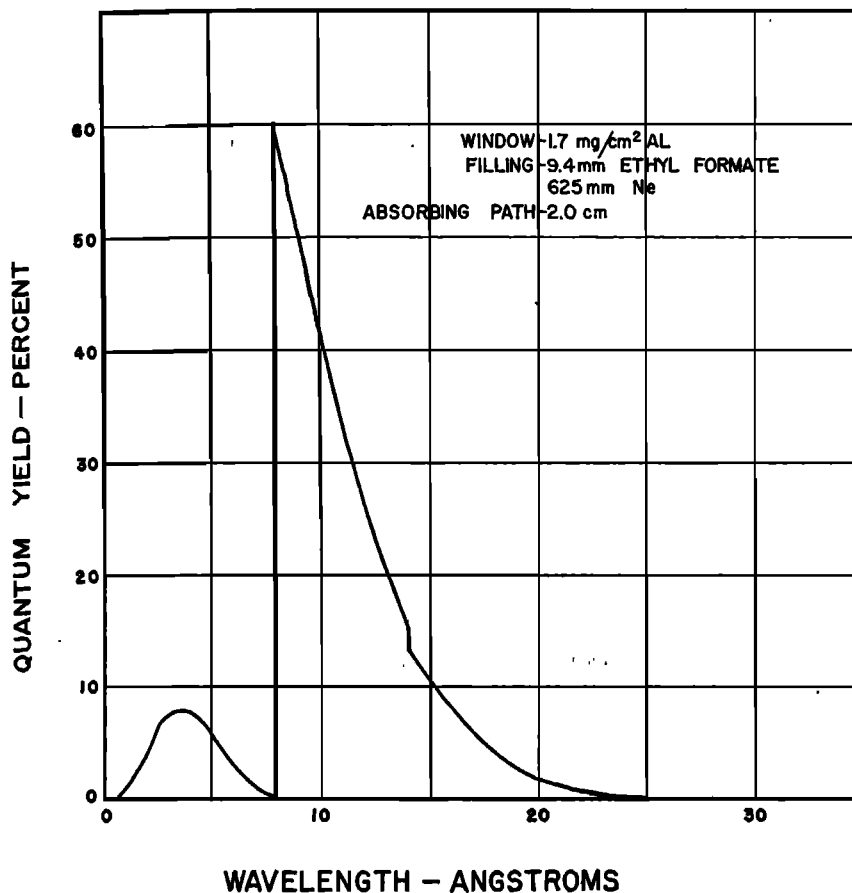


Fig. 1—Spectral sensitivity of photon counter with aluminum window. Discontinuities at 8 and 14Å are due to Al and Ne K edges.

About 37 percent of the electrons liberated at the cathode wall initiated counts. Since absorption of a 40Å x-ray quantum leads to the production of about 10 primary electrons, any one of which may initiate a count as it approaches the anode, each x-ray quantum absorbed must be better than 99 percent efficient in triggering a count.

In calculating the counter sensitivity curves of Figures 1 and 2, from 0 to 100Å, the absorption coefficients of Victoreen [6] were used on the short wavelength side of the K edge. These data were applied to hydrogen, helium, and beryllium over the entire range and to carbon below 43.5Å, nitrogen below 31Å, oxygen below 23.5Å, and neon below 14.0Å. Absorption coefficients for aluminum, for carbon above 43.5Å, O₂ above 23.5Å, and Ne above 14.0Å were obtained from Jonsson's [7] universal absorption curve, adjusted to pass through S. J. M. Allen's [8] values measured at the carbon K emission line at 44.5Å. The surface densities of the thin windows which were flown were determined by weighing portions of the larger sheets of aluminum and Mylar from which they were cut. The same procedure was followed for Glyptal films, but since they were cast on cleaved rock-salt plates of small area, the windows which were flown could not be cut from

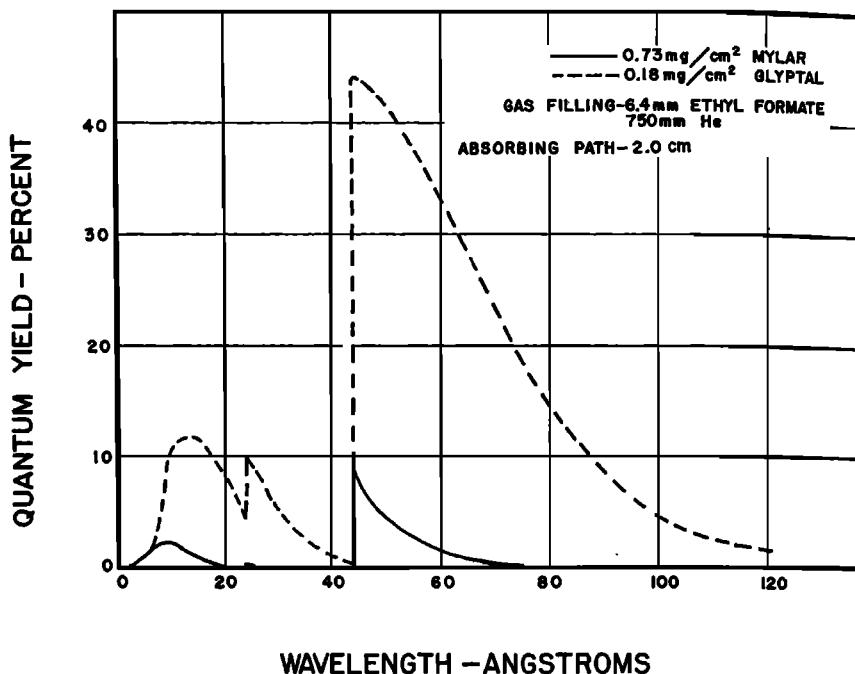


FIG. 2—Spectral sensitivities of photon counters with Mylar and Glyptal windows. Discontinuities at 22 and 43A are due to oxygen and carbon K edges. Mylar is Dupont Polyester film. Glyptal is a General Electric Company alkyd resin.

the same films that were weighed. Using the optical transmission of each Glyptal film at 2725A as a gauge of thickness, all films used in preparing counter windows were maintained within 30 percent of the optical density of the weighed film. The atomic composition of Glyptal is similar to that of Mylar, which has the composition $(C_{10}H_8O_4)_x$.

To obtain an experimental check on the relative sensitivities of different tubes, each photon counter was exposed to the continuum of x-radiation generated in a tungsten target tube, operated at voltages in the range of 50 to 2000 volts. The photon counter was clamped to a windowless aperture of the continuously pumped x-ray tube. It was assumed that the x-ray spectral distribution was given by Kramer's law,

$$N(\lambda, V) d\lambda = K \cdot \frac{1}{\lambda} \left(\frac{V}{12,400} - \frac{1}{\lambda} \right) d\lambda \dots \dots \dots (1)$$

where N is the number of quanta per second at wavelength λ , V is the accelerating voltage, and K is an experimental constant. From the observed response of a counter under test as a function of voltage, the shape of its spectral sensitivity curve was calculated. The spectral sensitivity curves determined in this way agreed well with the theoretical curves for those detectors which were sensitive only to wavelengths shorter than about 40A. Some disagreement was noted in the case of detectors sensitive to longer wavelengths. The observed sensitivity appeared to fall off somewhat too rapidly at long wavelengths and excessive response was indicated in the 30-40 region. This behavior most likely was due to deposition of

carbon on the x-ray tube target, with the accompanying emission of carbon K lines and suppression of the longer wavelength continuum. The theoretical sensitivity curves were used in all the computations described in this paper. The experimental calibrations gave accurate relative sensitivities of similar tubes with different window areas and qualitative checks on the long wavelength limits of response.

Experimental Results

Although solar x-rays had been detected by photon counters in five different previous rocket experiments, Aerobee 16 was the first flight that yielded information about the spectral distribution at longer x-ray wavelengths. Observed responses of tubes equipped with aluminum, Mylar, and Glyptal windows are shown in Figure 3. These data were corrected before plotting for dead-time losses

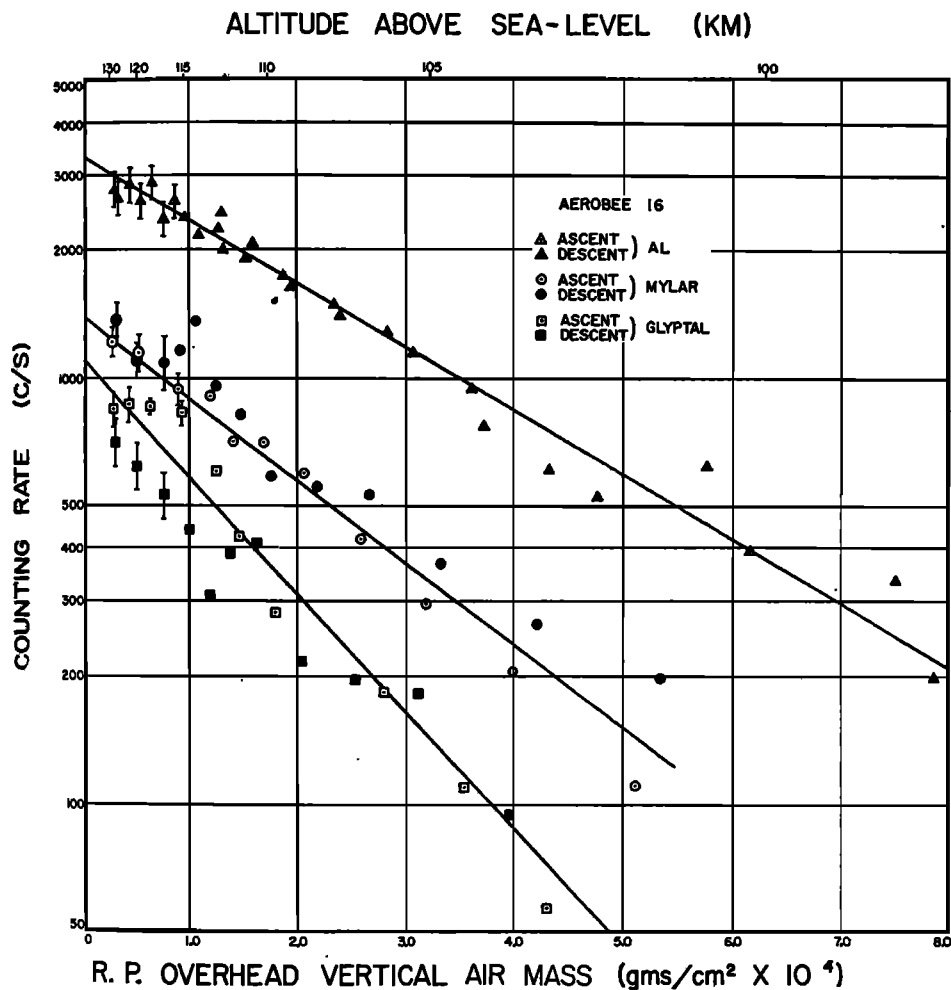


FIG. 3—Counting rates corrected for aspect and dead time plotted *versus* altitude and Rocket Panel residual air mass. To show the three curves in the same Figure, the ordinates of the Glyptal curves have been divided by two.

and for aspect, the angle between the normal to the counter window and the direction of the sun. Aspect was obtained from photocells and the appropriate corrections were determined from measurements in the laboratory of x-ray response versus angle of incidence. The peak intensities extrapolated to zero air path and the magnitudes of the applied corrections are listed in Table 1.

TABLE 1—Basic counting rate data

Window } mg/cm ² }	{ Aluminum 1.6	Mylar 0.73	Glyptal 0.18
Aperture diameter.....	0.12 inch	0.010 inch	0.0053 inch
*Maximum dead-time correction.....	52%	14%	18%
*Aspect correction, ascent up to 1 km from peak	12 to 21%	14 to 32%	12 to 26%
*Maximum aspect correction.....	53%	69%	64%
*Extrapolation of count rate to zero air path..	12%	11%	18%
**Transmission of gauze attenuator.....	32%
Counts/cm ² sec, zero air path.....	4.5×10^4	2.8×10^6	4.9×10^7

*All corrections are given in percentage of corrected value.

**Measured in ultraviolet.

To obtain the total intensity of solar x-ray emission from the responses of these narrow-band counter tubes, it is necessary to know the shape of the solar x-ray spectrum. It is interesting to estimate the energy in the incident x-ray spectrum, when we approximate the coronal emission by a grey-body distribution with the temperature and total energy as variable parameters. Results of calculations for temperatures of 7×10^5 , 10^6 , and 2×10^6 deg K are shown in Table 2. A grey-body emission curve of the indicated temperature was assumed, and the total intensity was adjusted to give the observed counting rate for each tube.

TABLE 2—Conversion of counting rates to x-ray intensities

Aerobee rocket	NRL 16	NRL 16	NRL 16	NRL 14
1. Tube window.....	Aluminum	Mylar	Glyptal	Glyptal
2. *Counts/cm ² sec.....	4.5×10^4	2.8×10^6	4.9×10^7	5.9×10^8
3. Peak quantum yield of counter.....	60%	9%	44%	44%
4. Limits of spectral response (Angstroms).....	8 to 20	44 to 60	44 to 100	44 to 100
5. Ergs/cm ² sec within limits of spectral response:				
7×10^5 deg K.....	0.00074	0.023	0.053	0.064
1×10^6 " ".....	0.00069	0.021	0.042	0.051
2×10^6 " ".....	0.00039	0.014	0.029	0.035
6. Ergs/cm ² sec in total x-ray spectrum:				
7×10^5 deg K.....	0.094	0.099	0.10	0.12
1×10^6 " ".....	0.011	0.11	0.12	0.14
2×10^6 " ".....	0.00085	0.24	0.29	0.35

*Extrapolated to top of atmosphere.

Row 5 of Table 2 gives the intensity within the narrow wavelength limits of tube response; row 6 lists the total intensity in the grey-body distribution. Thus, we can see that a 700,000 deg K distribution containing $0.1 \text{ erg cm}^{-2} \text{ sec}^{-1}$ fits the observed counting rates of all three types of counter. The emissivity of such a grey body is about 4×10^{-16} . At the higher temperature of 10^6 deg K, the total intensity computed on the basis of the Al tube differs by a factor of ten from that based on the Mylar or Glytal tubes. This wide difference in total intensity illustrates the sensitive dependence of the calculation on the assumed temperature, in spite of the fact that the intensities within the narrow bands of detection, row 5, vary comparatively little.

Aerobees 14 and 16 were flown during a period when solar activity was at a minimum. It may be concluded from the above discussion that the total x-ray intensity computed from observations in the neighborhood of 50A on the basis of a 7×10^5 to 10^6 deg K distribution is probably a good value for a quiet sun. It would be a great oversimplification, however, to attempt to assign a single temperature and emissivity to an active sun. When small patches of the corona become active, the short wavelength limit of the spectrum may be profoundly affected, while the 50A region remains comparatively constant and indicative of the major portion of the x-ray flux from the entire coronal disk. An apparent temperature of 7×10^5 deg K for the spectral distribution of a quiet sun as derived from the data of Aerobee 16 agrees roughly with the mean temperatures of 7×10^5 to 8×10^5 deg K deduced from radio noise measurements of the inner corona. Doppler widths of the coronal green and red lines indicate higher temperatures, which may be due to turbulent motions of the active regions within which these lines are most intense.

Coronal Fluctuations

Several authors have discussed the problem of x-ray emission from the corona, but the most detailed analysis has been carried out by Elwert [9]. In the preceding discussion, the experimental data were compared with grey-body distributions. Since the corona is optically thin in x-ray wavelengths, it is obvious that a grey-body distribution can only be an approximation. Elwert computed the recombination spectrum of electrons and highly stripped ions and the emission due to free-free transitions. The resulting spectrum closely resembled a Planckian distribution, with the maximum occurring at about 30A for an assumed 10^6 deg coronal temperature. A subsequent calculation of line emission excited by electron impact and by capture into excited states showed that line emission contributes the greater portion of the total x-ray radiation and that the maximum of the line distribution is centered about 60A for $T = 10^6$ deg K.

Elwert's calculations were based on an isothermal and homogeneous corona. In reality, there is considerable evidence that the corona shows marked density and temperature fluctuations in the neighborhood of active centers. For example, such fluctuations are necessary to explain the simultaneous appearance of the FeX(IP = 233 eV) red line and the FeXIV(IP = 355eV) green line in the same coronal region, even though their ionization potentials, IP, and therefore the ionization temperatures must differ greatly.

Minnis [10] found a very clear correlation between the ionization of the *E* and *F* regions of the ionosphere and the obscuration of active coronal patches during the progress of an eclipse. During the eclipse of February 25, 1952, the level of solar activity was comparatively high, and 36 percent of the ionizing radiations was observed to originate in clearly defined sources of intense green-line (FeXIV) emission. It seems quite reasonable to conclude that the active coronal centers are regions of higher temperature and density, with which are associated an enhanced x-ray emission shifted in the short wavelength direction.

An examination of rocket data for the 0 to 20A region and intensities of coronal emission lines at the times of flight lends further support to the above picture. Beginning with the first exploratory flight in 1949, six flights which carried x-ray sensitive Geiger counters to altitudes adequate for observing incoming x-rays have now been analyzed. Although none of the rocket flights coincided with observed flares, the activity of the sun as observed in coronal emission lines varied considerably. The firing dates, counter types flown, and responses are tabulated in Table 3, together with a set of numbers which represent the intensity of three visible coronal lines at the time of the flights. Since the coronal lines are measured only at the limbs of the sun by the coronagraphs at Sacramento Peak and at Climax, the condition of the visible disk at the time of firing was approximated by averaging the intensities observed at the east limb of the sun over the seven days previous to a rocket firing with the intensities at the west limb of the sun over the seven days following the rocket firing. The intensity numbers in Table 3 are proportional

TABLE 3—Fluctuations in short wavelength x-ray emission and coronal line intensities

Rocket	V-2 #49	Aerobee 9	Aerobee 10	Viking 9	Aerobee 14	Aerobee 16
1. Date of firing.....	9/29/49	5/1/52	5/5/52	12/15/52	11/15/53	12/1/53
2. Counter window.....	Be	Be	Be	Al	Al	Al
	13 mg/cm ²	47 mg/cm ²	47 mg/cm ²	1.59 mg/cm ²	1.59 mg/cm ²	1.59 mg/cm ²
3. Counts/cm ² sec (a).....	1.0 × 10 ⁴	495	<125	2.9 × 10 ⁶	<3.1 × 10 ⁴	4.5 × 10 ⁴
4. Limits of spectral response (Angstroms).....	7 to 12	5 to 9	5 to 9	8 to 20	8 to 20	8 to 20
5. Ergs/cm ² sec, 0 to 20A (b):						
10 ⁶ deg K.....	0.44	2.5	<0.04	0.2	<0.0015	0.0007
2 × 10 ⁶ deg K.....	0.01	0.0034	<0.0009	0.2	<0.0015	0.0004
6. Intensity of coronal lines:						
FeX 6374A, IP = 238 eV.....	(d)	104 (c)	109 (c)	131	136	131
FeXIV 5302.9A, IP = 355 eV....	(d)	227 (c)	254 (c)	224	68.1	85
NiXV 6702A, IP = 422 eV....	(d)	26 (c)	32 (c)	25	0.5	0
CaXV 5694.4A, IP = 814 eV....	(d)	0	0	0	0	0

(a) Extrapolated to top of atmosphere.

(b) Viking 9 and Aerobee 14 were filled with helium and quench agent; all others were filled with neon and quench agent.

(c) Coronagraph data given lower statistical weight due to poor conditions of observation.

(d) No coronagraph data available.

to the average values obtained at Sacramento Peak, weighting equally all intensities obtained between -60° and $+60^\circ$ solar latitude. The data used in these computations were obtained from Central Radio Propagation Laboratory Reports of the National Bureau of Standards on "Ionospheric Data." The intensity data of row 5 were computed for two temperatures, 10^6 and 2×10^6 deg K. If a lower

temperature such as 7×10^5 deg K were used, the resulting computed intensities for the Be window tubes would have been impossibly large.

It seems clear that the larger quantities of x-ray flux below 20A observed in the Aerobee 9 and Viking 9 flights compared to the Aerobee 14 and 16 flights, are associated with increased intensities of the coronal lines arising from the most highly stripped ions. Row 6 shows that the intensity of the coronal red line (FeX) was fairly constant for all flight times. The intensities of the lines arising from higher ionization states of Fe and Ni were markedly higher during the Aerobee 9 and Viking 9 flights than during the Aerobee 14 and 16 flights. These results suggest further that a strong flux of x-rays capable of penetrating below *E* layer might be present during periods when the coronal Ca yellow line (IP = 814 eV) is observed.

As we approach the maximum of the sunspot cycle in 1958, rocket experiments will have a much greater probability of observing x-ray emission from centers of high coronal activity. It would be interesting to fire a sequence of rockets during the progress of an eclipse to define the distribution of coronal x-ray sources, as Minnis has done with ionosphere measurements. Suitable small rocket techniques now being perfected should make such an experiment entirely feasible for the eclipse of October 12, 1958.

Atmospheric Density in the E Region

Atmospheric pressure has been one of the most frequently measured parameters of rocket experiments at high altitudes. A report of the Rocket Panel [11] summarizes the results obtained up to 1952. From 76 cm down to a few centimeters of pressure, bellows gauges have yielded data which are considered correct to within 10 percent. In the ranges 2 mm to 3×10^{-3} mm and 10^{-2} mm to 10^{-6} mm, measurements have been made with Pirani and Philips gauges, respectively. It is recognized that these latter measurements could be in error by a factor of two in *E* region due to outgassing and yawing of the rocket. Gases escaping from the rocket's powerplant, interior, and surface may exceed the atmospheric pressure at higher altitudes.

By measuring the rate at which the incident x-ray flux increases with altitude in the *E* region, one can deduce the variation in overhead air mass with altitude. This method of measuring atmospheric density can be only negligibly affected by gas in the immediate vicinity of the rocket, since the observed x-ray absorption is determined by changes in the total air path between the missile and the sun. The method is strictly accurate only for detectors of quite narrow spectral response, because of the great variation of x-ray absorption coefficients with wavelength. The mass absorption coefficients of air at N.T.P. are shown in Figure 4. The lengths of the horizontal bars represent the effective limits of spectral response of photon counters employed in Aerobee 16, namely, aluminum, 8 to 20A, Mylar, 44 to 60A, and Glyptal, 44 to 100A, with the exception of the bar marked "4900," which will be explained. It is clear that each counter embraced a spectral region over which the mass absorption coefficient varies appreciably with wavelength.

The counting rate observed in each of these counters as a function of altitude is plotted in Figure 3. The lower abscissa represents the total mass of air in a one cm^2 vertical column between the rocket and the top of the atmosphere, the value for any altitude being computed from the density tables published by the Rocket

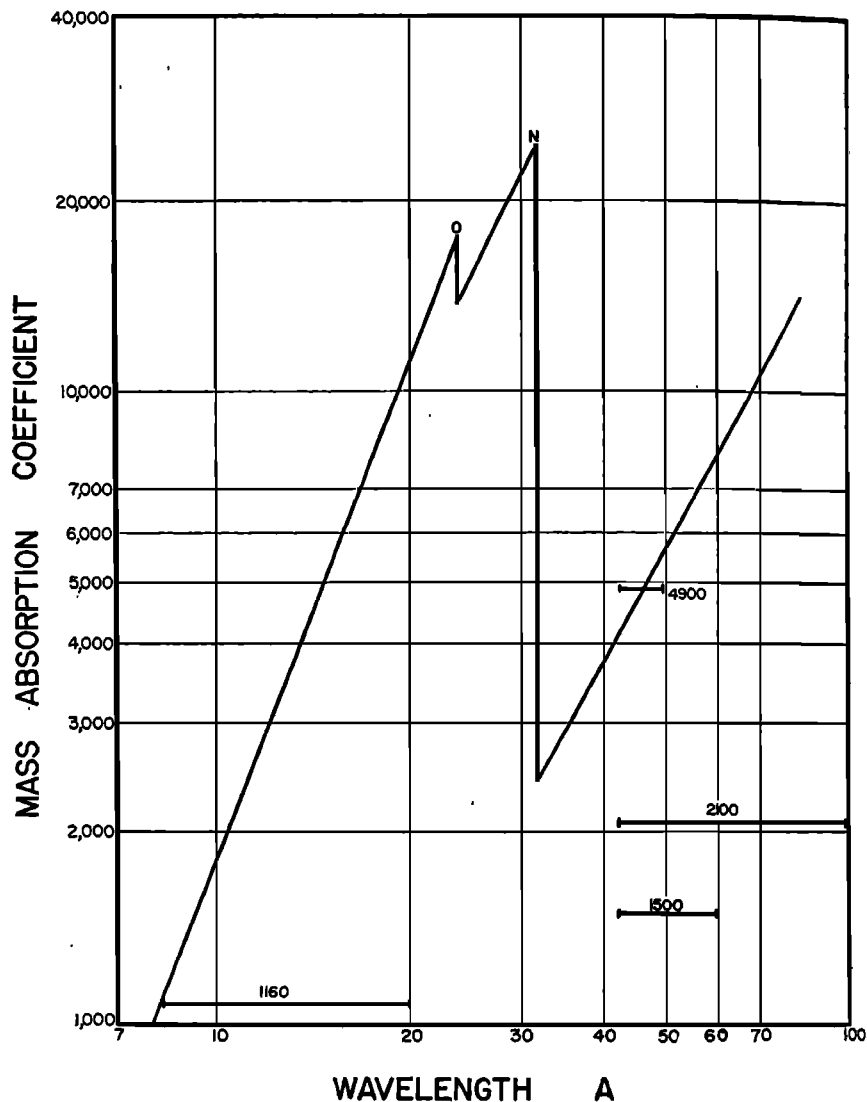


FIG. 4—X-ray absorption coefficient of standard air *versus* wavelength. The horizontal bars span the wavelength limits of spectral response of the three photon counters flown in the rocket and one tube used in the laboratory measurement.

Panel [11]. At the time of the rocket flight, the sun elevation was $17^{\circ} 35'$, corresponding to a slant air path of 3.3 atmospheres between the rocket and the sun. The slopes obtained from the log counting rate *versus* slant air mass are the mass absorption coefficients for air, $1160 \text{ cm}^2/\text{gm}$, $1500 \text{ cm}^2/\text{gm}$, and $2100 \text{ cm}^2/\text{gm}$, in the spectral regions measured by counters with aluminum, Mylar, and Glyptal windows, respectively. These absorption coefficients are represented by the ordinates of the horizontal bars in Figure 4. They fall well below the known absorption curve for air; that is, the results indicate that there was, in fact, less air above the

rocket at any altitude than the abscissae of Figure 3 show. To check the validity of this conclusion, the absorption coefficient of air was measured in the laboratory with a Mylar photon counter and an x-ray tube operating at 500 volts. By using additional Mylar filtration, the response of this counter was made even narrower than that of the tube actually flown in the rocket. The mass absorption coefficient of air so obtained was $4900 \text{ cm}^2/\text{gm}$. This value is also plotted in Figure 4, and it is seen to fit the curve. The length of the bar shows the reduced spectral band width of this measurement.

Since the laboratory measurement gave the correct absorption coefficient, the fact that the rocket results all fell below the true curve was attributed to incorrectness of the abscissae of Figure 3, taken from the Rocket Panel Report. The present rocket results would yield the correct absorption coefficients if Figure

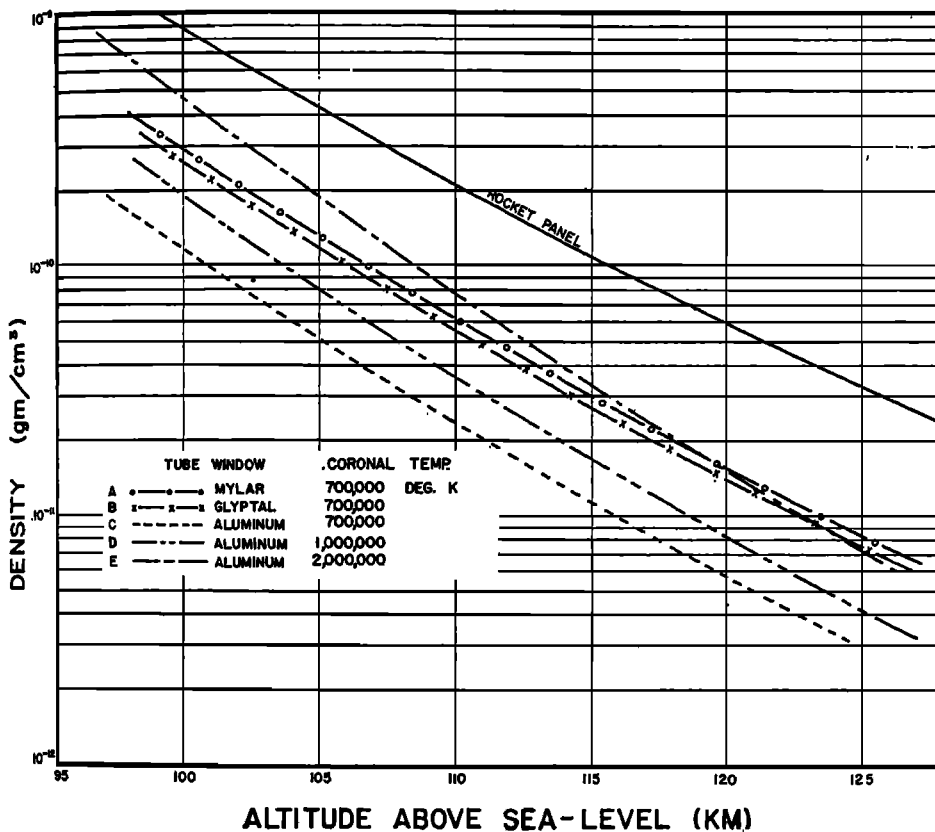


FIG. 5—Density of air versus altitude

3 were replotted using one-half to one-tenth the R.P. values for air density. Figure 5 shows several curves of the variation of air density with altitude in the 100- to 128-km region, derived from the rocket data of Figure 3, using the known values of x-ray absorption coefficients for air. The density curve of the Rocket Panel Report of 1952 lies above all the experimental curves. Curve A was derived from

the response of the Mylar window tube flown in Aerobee 16. Curves *B* and *C* are the corresponding data for the Glyptal and the aluminum windows. The choice of spectrum, 7×10^5 to 2×10^6 deg K grey body, has a pronounced effect on the densities computed from the aluminum tube response. This is attributed to the fact that the aluminum tube is sensitive to a spectral band on the short wavelength side of λ_{\max} of the Planckian distributions, where the slope of the spectral emission curve is very steep. On the other hand, the densities based on the Mylar and Glyptal tube responses are almost unaffected by the choice of grey-body emission temperature. The sensitivities of these tubes are mainly confined to bands on the long wavelength side of λ_{\max} , where the emission of the Planckian distribution varies slowly with wavelength. The slight sensitivity of the Mylar and Glyptal tubes below the carbon K edge contributes an insignificant amount to the total counting rate. Basing the computed density on the Mylar tube data, the x-ray values for the Aerobee 16 flight (10:00 AM, MST, Dec. 1, 1953) are about one-third the R.P. densities at altitudes between 110 and 128 km.

The density *versus* altitude curves of Figure 5 emphasize the inadequacy of a single temperature grey-body approximation to the coronal x-ray spectrum. Earlier in the paper, we showed that a 7×10^5 deg K grey body emitting a total intensity of $0.1 \text{ erg cm}^{-2} \text{ sec}^{-1}$ provided a good fit to the intensities measured by the three different photon counters. The density data of Figure 5, however, require that the solar emission in the 8A to 20A band covered by the aluminum tube be characterized by a temperature of 1.5×10^6 to 2×10^6 deg K. A narrow band of emission peaking at 13A would fit still better. The flux density at 2×10^6 deg K required to produce the counting rate of the aluminum tube would increase the counting rates of the Mylar and Glyptal tubes by less than one percent. If at the same time the coronal regions responsible for radiation in the 44A to 100A band were characterized by a temperature of 5×10^5 deg K, the short wavelength contribution below 20A from these regions would be negligible. A combination of such hot and cold regions could readily account for a total intensity of $0.1 \text{ erg cm}^{-2} \text{ sec}^{-1}$ with the observed spectral composition.

The x-ray method of density determination utilizing the 50A region of the spectrum is limited to the *E* region of the ionosphere if the sun is near the zenith. At sunrise and sunset, the slant air path may be increased sufficiently to extend the measurements to *F*1 region. The least penetrating solar radiation, that which is absorbed at the highest altitudes, is contained in the broad spectral region between 200A and 1200A. Laboratory measurements of air absorption in this part of the spectrum show that the absorption coefficients lie within the range 300 to 1000 cm^{-1} (base *e* at N.T.P.) A broad band detector could, therefore, be utilized to determine density within a factor of roughly two in *F*2 region. Such a detector can be prepared in the form of a free-flow windowless counter with high quantum efficiency over the entire spectrum from 10 to 1200A, the latter value being the ionization threshold of the counter gas. Preliminary experiments with such tubes have demonstrated that the response to longer wavelength solar ultraviolet can be identified by its appearance at low altitudes and that it contributes a small counting rate compared to the shorter wavelengths encountered above 100 km. Future experiments in the Aerobee-Hi are expected to reach 180 miles and will

permit density determination from observations of solar UV and x-ray absorption up to the maximum altitudes at which such radiations are absorbed.

The authors are indebted to J. J. Nemecek and W. A. Nichols for valuable assistance in the design and execution of the experiments.

References

- [1] H. Friedman, S. W. Lichtman, and E. T. Byram, *Phys. Rev.*, **83**, 1025 (1951).
- [2] E. T. Byram, T. A. Chubb, and H. Friedman, *Phys. Rev.*, **92**, 1066 (1953).
- [3] F. S. Johnson, J. D. Purcell, H. H. Malitson, and R. Tousey, *Astr. J.*, **60**, 165 (1955).
- [4] W. A. Rense, *Phys. Rev.*, **91**, 299 (1953).
- [5] E. T. Byram, T. A. Chubb, and H. Friedman, *Phys. Rev.*, **98**, 1594 (1955).
- [6] J. A. Victoreen, *J. Appl. Phys.*, **20**, 1141 (1949).
- [7] E. Jonsson, Thesis, Upsala (1928); M. Siegbahn, "Spektroskopie der Röntgenstrahlen," J. Springer, Berlin (1931), p. 470.
- [8] S. J. M. Allen, "X-rays in theory and experiment" by A. H. Compton and S. K. Allison, p. 799 (1943).
- [9] G. Elwert, *Zs. Naturf.*, **9a**, 637 (1954).
- [10] C. M. Minnis, *J. Atmos. Terr. Phys.*, **6**, 91 (1955).
- [11] The Rocket Panel, *Phys. Rev.*, **88**, 1027 (1952).